

# Effect of nintedanib thermo-sensitive hydrogel on neovascularization in alkali burn rat model

Yan Gong, Guo-Hai Wu, Ling-Yi Zhang, Zhe Zhang, Yan-Hong Liao, Xiao-Tian Liu

Department of Ophthalmology, Ningbo Eye Hospital, Ningbo 315040, Zhejiang Province, China

**Correspondence to:** Yan Gong and Xiao-Tian Liu. Department of Ophthalmology, Ningbo Eye Hospital, No.599 North Mingcheng Road, Ningbo 315040, Zhejiang Province, China. 18906627688@189.cn; 523755781@qq.com

Received: 2020-01-14 Accepted: 2020-04-13

## Abstract

• **AIM:** To investigate the effects of nintedanib thermo-sensitive hydrogel (NTH) on neovascularization and related markers in corneal alkali burns of Wistar rats.

• **METHODS:** NTH was prepared by grinding, and its phase-transition temperature was determined. Thirty specific-pathogen-free Wistar rats served as a model of corneal alkali burn in the right eye were randomly divided into 3 groups ( $n=10$ , each): model group treated with 0.9% saline once a day, NTH group with 0.2% nintedanib *b.i.d.*, and dexamethasone group with dexamethasone ointment once a day. The left eye of rats served as the controls. The corneal transparency was observed under a slit-lamp microscope, and the area of neovascularization was calculated. On day 7, the rats were sacrificed, and the cornea was removed and embedded with paraffin, then stained with hematoxylin-eosin, and the expression of vascular endothelial growth factor receptor 2 (VEGFR-2) and CD31 in the corneal tissues of each group was detected by immunofluorescence.

• **RESULTS:** The phase-transition temperature of nintedanib obtained by grinding was 37°C after adding artificial tears. The results of the alkali burn model indicated that the growth rate of neovascularization in the NTH group was slower than that in the model group, and the neovascularization area was significantly smaller than that in the model group ( $P<0.05$ ). Moreover, CD31 and VEGFR-2 expression levels in the NTH group were significantly lower than those in the model group.

• **CONCLUSION:** NTH becomes colloidal at body temperature, which is beneficial for releasing the drug slowly and can significantly inhibit the neovascularization of corneal induced by alkali burn in rats.

• **KEYWORDS:** nintedanib; alkali burn; neovascularization; cornea; rat

**DOI:10.18240/ijo.2020.06.04**

**Citation:** Gong Y, Wu GH, Zhang LY, Zhang Z, Liao YH, Liu XT. Effect of nintedanib thermo-sensitive hydrogel on neovascularization in alkali burn rat model. *Int J Ophthalmol* 2020;13(6):879-885

## INTRODUCTION

There are no blood vessels in the normal corneal tissue, and the non-vascularization of the cornea is one of the essential factors to maintain its transparency. Corneal neovascularization (CNV) is formed by the invasion of the cornea from the limbal vascular network under the various toxic stimuli such as hypoxia, inflammation, and injury<sup>[1]</sup>. CNV often leads to loss of transparency of the cornea, causing impaired vision and even blindness. It is also a high-risk factor for corneal transplant rejection. So far, there is little convenient and effective CNV treatment in clinical practice. Screening for the anti-CNV drug is mainly based on various animal models, of which the most commonly used is the rat's alkali burn model. In brief, alkali was applied on the surface of the rat eyes, and the corneal epithelium would be missing after alkali burn<sup>[2]</sup>. Under the action of inflammatory factors, the neovascularization is caused from the limbus. It grows in the direction of the cornea and forms CNV. In this process, vascular endothelial growth factor (VEGF) plays a vital role by binding to the vascular endothelial growth factor receptor (VEGFR). The VEGF-targeted antibody or antagonizing VEGFR will postpone the progression of CNV to some extent; nevertheless, approximately 25% of eyes in anti-CNV treatment show fibrosis within 2y<sup>[3-4]</sup>. At present, VEGF inhibitor or antagonist, such as conbercept, is mainly administered by injection, which made limited medication compliance, also placed the patients under great economic pressure<sup>[5]</sup>. Therefore, the development of a more cost-effective, more comfortable to administer drug would be the main direction in corneal CNV therapeutic.

Nintedanib is a newly marketed drug for the treatment of idiopathic pulmonary fibrosis<sup>[6]</sup>, which is a VEGFR-2 tyrosine kinase inhibitor and was originally developed for the

treatment of various cancers<sup>[7]</sup>. A recent study has shown that nintedanib eye drop could attenuate the formation of CNV in mice model<sup>[8]</sup>. However, the eye drops may not have long-term efficacy due to rapid elimination. In recent years, a new type formulation, thermo-sensitive hydrogel appears to solve this problem. Thermo-sensitive hydrogel is a temperature-sensitive hydrogel that can transform to gelatinous after being applied to local tissue. It is hydrophilic, sustained-released, and biocompatible, especially in mucosal tissue<sup>[9]</sup>. Also, it is suitable for the treatment of eye diseases. This study aimed to investigate the effect of NTH on neovascularization by establishing a rat corneal alkali burn model.

## MATERIALS AND METHODS

**Ethical Approval** The present study was performed in accordance with the Guide for the care and Use of Laboratory Animals published by the National Institutes of Health, and was approved by the Animal Care and Use Committee of School of Medicine of Ningbo University (No.2019C50059).

### Preparation of Nintedanib Thermo-Sensitive Hydrogel

The method was modified based on the previous study<sup>[10]</sup>. Nintedanib drug powder was slowly added into deionized water, stirred and dissolved on a magnetic stirrer. Poloxamer 407 (P407) was grinded into a fine powder, which was then slowly added to deionized water and stirred while adding. After the nintedanib dissolved completely, it added to the P407 solution and mixed. After adding the deionized water, the mixture was stirred on a magnetic stirrer to fully dissolved, which would look creamy ultimately. The pH of solution was adjusted to a range of 5-9, then the solution was chilled at 4°C until the P407 was completely dissolved (about 24-48h). The gelation temperature was measured after adding the artificial tear, which was composed of 6.78 g sodium chloride, 2.18 g sodium bicarbonate, 1.38 g potassium chloride, and 0.084 g calcium chloride dihydrate in 1 L deionized water.

**Measurement of the Gelation Temperature of Thermo-Sensitive Hydrogel** The improved “stirring method” was used to determine the sol-gel transition temperature<sup>[11]</sup>. In brief, about 7 mL of the gel matrix was placed in a fixed size (4×2 cm<sup>2</sup>) glass vial. The thermometer was inserted, and the mercury ball was completely immersed in the solution. Meanwhile, a stirrer of fixed size (7×3 mm<sup>2</sup>) was placed in the vial. The vial was placed in a water bath at a low temperature (the initial temperature at 5°C). The stirring rate (200 r/min) was adjusted and fixed. The water bath was heated at a rate of 0.5°C/min. The temperature of stirring stopping time (the time when the stirrer takes a turn for more than 3s) is the gelation temperature T1. The artificial tears were dropped into the 6 mL gel matrix gel at the proportion of tears:gel=7:40. The composition of the artificial tears was 6.78 g sodium chloride, 2.18 g sodium bicarbonate, 1.38 g potassium chloride, 0.084 g calcium chloride

dihydrate in 1 L of deionized water. The above processes were repeated under the same condition to obtain a gelation temperature T2.

**Rat Alkali Burn Model** Thirty Wistar male rats were purchased from Shanghai SLAC Laboratory Animal Co., Ltd., weighing 150-200 g, which were healthy without eye diseases. An alkali burn model was made after one week of adaptive feeding. The 4 mm diameter filter paper was immersed in 1 mol/L NaOH for 1min to make it saturated (normal saline was immersed in the control group for 1min). Rats were anesthetized with 4% chloral hydrate at the 45 mg/kg intraperitoneally. The 0.5% lidocaine was dropped on eyes, and rats underwent local anesthesia for 10s. Cotton swabs were used to remove excess liquid. Then the filter paper was placed in the center of the rat cornea for 20s. After the removal of the filter paper, the conjunctival sac was washed with normal saline for 1min. Burned rats were then randomly divided into 3 groups (10/group): chloramphenicol group (model group), 1% dexamethasone group, 0.2% nintedanib group, and normal control using the left eyes. The NTH was applied to the conjunctiva every day from the first day after the model was established. The rats in the remaining groups were given eye drops. Image J software was used to calculate the corneal neovascular area at 1, 3, 7, and 14d under the slit lamp microscope. The eyeballs were removed 14d after surgery, and sections were made. The rats received euthanasia by carbon dioxide in one transparent cage (keep in at least 30min).

**Observation of Neovascularization** At 3, 7, and 14d after modeling, the CNV was observed under the slit lamp microscope. The region of neovascularization was photographed, and the area was calculated. The length of the neovascularization from limbus to center was measured (the standard length is the length of blood vessels that is continuous, curved, and perpendicular to the tangential line of the limbus). The average value of each image was measured in five different quadrants to obtain the length of the CNV in different stages. The data were input into the Robert computer numerical model formula<sup>[12]</sup>, area (mm<sup>2</sup>)=0.2×π×VL (mm)×CN (mm), VL is the maximal vessel length of the neovascular, CN is clock hours of neovascularization, where 1 clock hour equals 30 degrees of arc. Image J software was used to calculate the ratio of corneal neovascular area to the total cornea.

**Immunofluorescence** The expression of VEGFR-2 and differentiation 31 (CD31) was detected by immunofluorescence. The eyeballs were formalin-fixed paraffin-embedded (FFPE) for immunofluorescent staining. In brief, the FFPE was sectioned into 4 μm. It was then dewaxed and rehydrated, repaired in an antigen retrieval solution above pH 9, and then blocked with 20% horse serum. The primary antibody was diluted with serum and incubated at 2°C-8°C overnight. A secondary

antibody (Alexa Fluor 488 labeled donkey anti-rabbit IgG, diluted 1:800), incubated at room temperature for 30min, observed under an upright fluorescence microscope, and photographed. Five fields were taken from each slide. IPP6.0 was performed to determine the relative value of positive immunofluorescence staining, which reflected the relative content of the labeled proteins in each group.

**Statistical Analysis** Each group of data was presented in the form of mean±SD of three independent experiments. The SPSS11.5 statistical analysis software was used for statistical analyses. The differences between the two groups were compared by the Student's *t*-test. The one-way variance analysis (ANOVA) was used to analyze the differences between multiple groups. A *P* value of <0.05 was considered to indicate a statistically significant result.

## RESULTS

**Physical and Chemical Parameters of Thermo-Sensitive Hydrogel** In this study, three different concentration of thermo-sensitive gels which containing different ratios of P407 and nintedanib were prepared (Figure 1). When the preparation was at 16°C, it can remain liquid, while the original temperature of gels changing into solid was 24°C. After adding artificial tears, the temperature of gels could reach 35°C, around the body temperature. We finally selected 0.2% nintedanib for the following experiments.

**Rats Corneal Neovascularization After Alkali Burn** In the alkali burn model group, the corneal epithelial edema in the injured area was observed 1d after modeling. The corneal sclera vessels were vasodilated and congested. After 4d, corneal neovascular buds appeared in the corneal sclera, and protruded into the transparent cornea. After 7d, the growth of corneal neovascular was exuberant. It became significantly longer and larger. The branches of blood vessels appeared which are partially anastomosed (Figure 2). After 14d, the CNV area reached the maximum which interlaced into a network and tended to be stable. CNV achieved stability after 21d. Some blood vessels disappeared. CNV in the nintedanib group was slower than that in the model group. The blood vessels did not reach the center, and the range was small, mostly confined to the corneoscleral margin. They did not interweave into a network (Figure 2). In the 0.2% nintedanib group, not only the growth length and range of the CNV were significantly smaller than those of the model group at various time points, but also the density was sparse, the blood vessels were fine, transparent, and the bifurcation was little (Figure 2).

**Area of Corneal Neovascularization** At 3, 7, and 14d after corneal alkali burn, the corneal neovascular area of each group was repeatedly measured and analyzed by variance analysis (Table 1). The data in the 0.2% nintedanib group at each time point was significantly lower than that in the model group

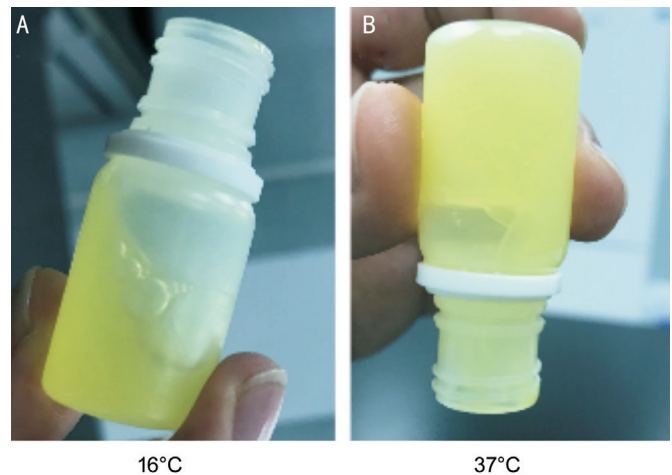


**Figure 1** The phase transition of thermo-sensitive gel after adding artificial tears A: The thermo-sensitive gel was a liquid in 16°C; B: The thermo-sensitive hydrogel underwent gelation in 37°C after adding artificial tears.

**Table 1** The CNV area of alkali burn rats at different time points

Groups	n	CNV area (mm <sup>2</sup> )		
		Day 3	Day 7	Day 14
Model	10	8.47±1.80	18.87±3.07	24.34±2.39
0.2% nintedanib	10	5.25±2.33 <sup>a</sup>	6.46±3.67 <sup>a</sup>	7.04±2.45 <sup>a</sup>
Dexamethasone	10	4.26±2.79 <sup>a</sup>	6.38±3.54 <sup>a</sup>	10.23±4.56 <sup>a</sup>
Normal control	30	24.55±3.63	22.73±3.98	25.36±2.75

Data were represented as mean±SD. <sup>a</sup>*P*<0.05, compared to model group.

(*P*<0.05). On day 3, the inhibition effect of neovascularization was observed in the 0.2% nintedanib group, suggesting that nintedanib thermo-sensitive gel took the effect quickly. The inhibition effect of nintedanib was as good as dexamethasone in the short term with significant difference (*P*<0.05). Moreover, its function was prolonged to 14d after modelling.

### Pathological Structure, CD31 and VEGFR-2 of Rat Corneal

The corneal hematoxylin-eosin staining showed that the typical layers of the corneal tissue were intact (Figure 3), the cells were tightly arranged, and no neovascularization was observed. The number of corneal neovascular at the corneal margin in the model group was more than that in other groups. The neovascular invaded into the corneal stroma. The neovascular lumen was visible in the stromal layer, where a large number of red blood cells attached. The capillaries at the corneoscleral margin in the dexamethasone and nintedanib group were dilated, and the number of neovascular lumens was small.

On the first day after modeling, the inflammatory cell infiltration was observed at the corneoscleral margin. The cytoplasmic VEGFR-2 staining was not obvious (data not shown). At day 3 after modeling, the green cytoplasmic fluorescent staining of VEGFR-2 was observed. On day 7,

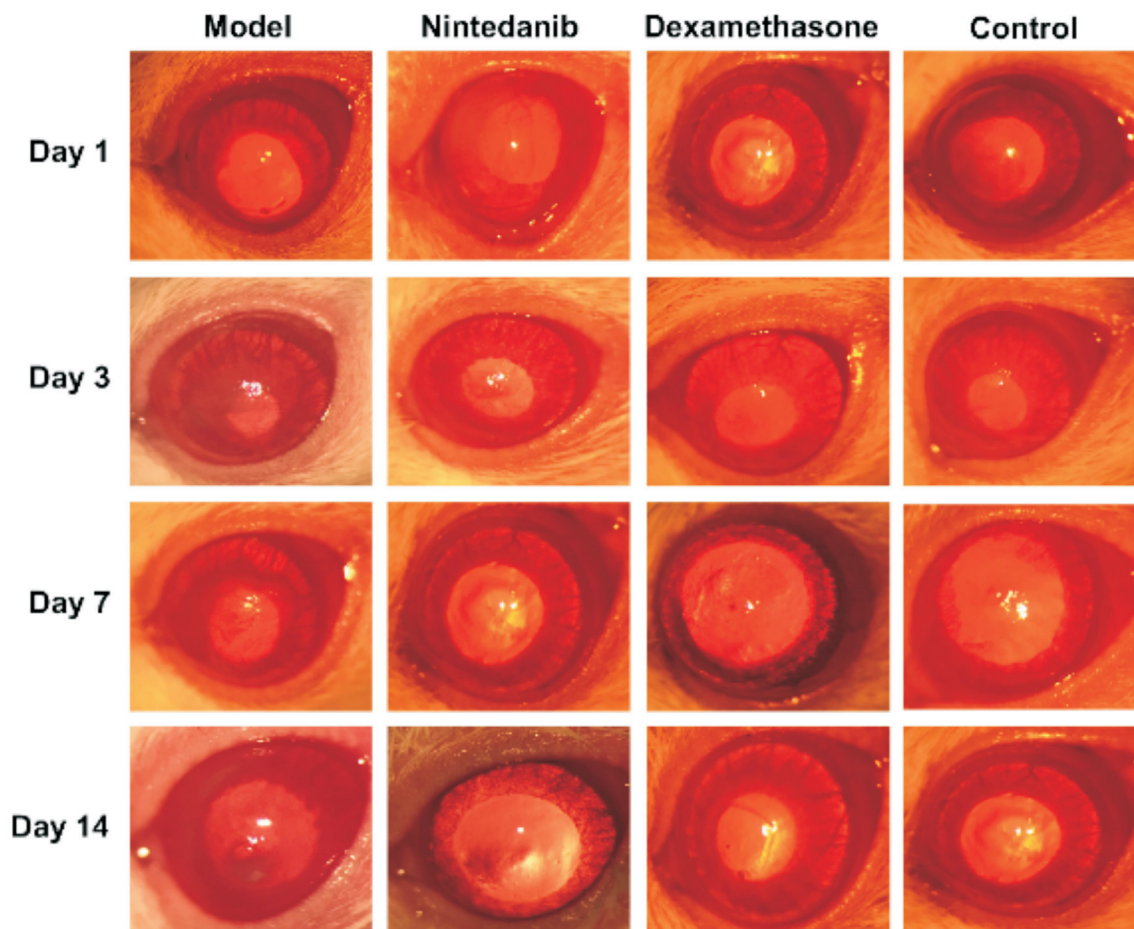


**Figure 2 Images of CNV after alkali burn at different time points** Representative gross images of eyes treated with chloramphenicol, 0.2% nintedanib, 1% dexamethasone and normal control at 1, 3, 7, 14d after alkali burn.

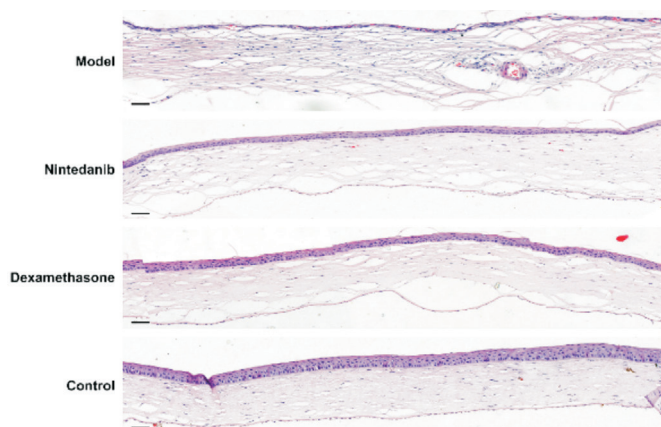


**Figure 3 Hematoxylin-eosin staining of corneal tissues** Representative hematoxylin-eosin staining of entire cornea treated with chloramphenicol, 0.2% nintedanib, 1% dexamethasone, and normal control at 7d after alkali burn. Scale bar=50  $\mu$ m.

the dark green staining of VEGFR-2 was shown in the shallow 1/3 stromal layer and the keratinocyte keratin. The inflammatory changes in the corneal stromal layer were apparent (Figure 4). At 14d after modeling, the dark green staining was presented in the cytoplasm of inflammatory cells in the stromal layer. However, the inflammatory changes in

the cornea were slight. In the nintedanib-administered group, the inflammatory cell infiltration of the cornea was mostly limited in the corneoscleral margin and the shallow stromal layer, and the number of cells was fewer than that in the model group. The cytoplasmic VEGFR-2 staining was lighter, and the inflammatory response was significantly reduced on the 7<sup>th</sup> day.

Subsequently, the expression of CD31 was detected (Figure 5). A cluster of CD31 is a platelet endothelial cell adhesion molecule (PECAM-1). It is a member of the immunoglobulin superfamily and is expressed in vascular endothelial cells, platelets, monocytes, neutrophils as well as many other cell surfaces, which indicates neovascularization. The fluorescein level of blood vessels was further evaluated by immunofluorescence. The results showed that the expression of CD31 in the corneal tissue was the lowest in healthy control rats. The expression was also significantly down-regulated in the nintedanib and dexamethasone-treated groups, while the expression was up-regulated significantly in the control group.

#### DISCUSSION

At present, the medical treatment of CNV is mostly in the experimental stage, and it is relatively rare in clinical

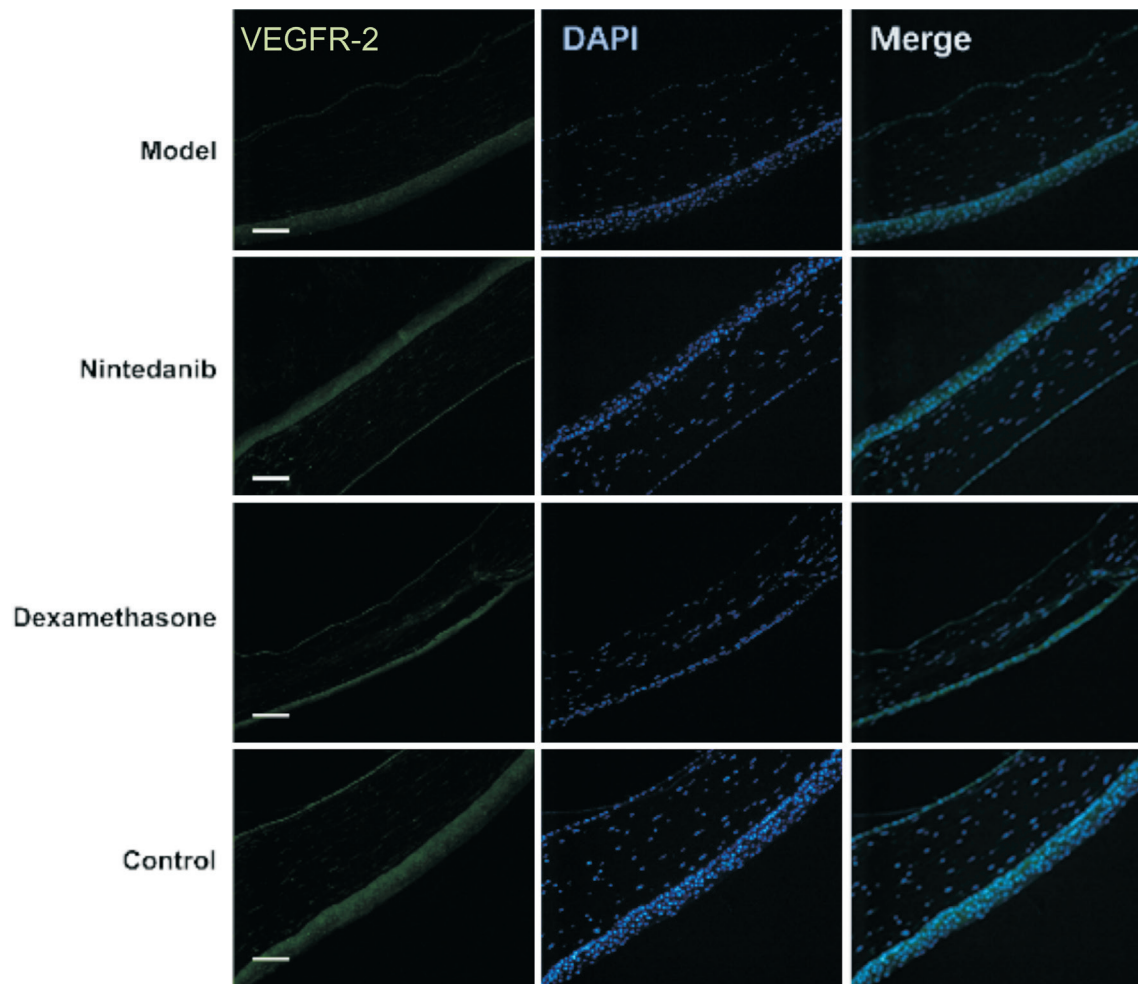


**Figure 4 Immunofluorescence of VEGFR-2** Representative VEGFR-2 staining images in model, 0.2% nintedanib, 1% dexamethasone, and normal control group at 7d after alkali burn. DAPI was used for nucleus staining. Scale bar=100  $\mu$ m.

application. There are no ideal methods for the treatment of corneal CNV, so it is crucial to develop a new treatment method to inhibit CNV occurrence and development. Traditional drug delivery to the eyes, such as eye drops and eye ointment, has certain limitations. For example, the eye drops eliminate quickly and cannot stay in the cornea for a long time. Eye ointment may affect vision due to uneven coating on the eyeball. The application of thermo-sensitive gel is expected to change this situation. Its main feature is temperature sensitivity. It is a liquid at room temperature or during cold storage<sup>[13]</sup>. After contacting with organ, the phase changes and becomes gelatinous due to the body temperature. In this way, the liquid can distribute evenly, and in the later stage, the viscosity of the gel is utilized to allow the drug to stay on the surface of the eye for a long time, which helps the drug to keep its effect sustainably<sup>[14-15]</sup>. Eye treatment using thermo-sensitive gel may be the most potential drug delivery mode in the future, which has the advantages of simplicity, convenience, and painlessness.

CNV is a common pathological phenomenon closely related to corneal chemical burns, corneal inflammation, and

corneal allograft rejection<sup>[1]</sup>. The mechanism of occurrence is complicated. At present, most researchers believe that it is related to the imbalance of their angiogenesis inhibitors and angiogenesis factors, which cause the angiogenesis factors to become dominant. VEGFR-2 is currently one of the most direct factors that promote intraocular neovascularization. Two tyrosine receptors, Flt-1 and Flk-1, which specifically act on the surface of vascular endothelial cells, are involved in vascular endothelial cell division, proliferation, and migration<sup>[15]</sup>. They stimulate the secretion of extracellular matrix by corneal stromal cells, increase vascular permeability, and promote neovascularization. We found that VEGFR-2 protein content and neovascular length changed synchronously at different stages after corneal alkali burn. It was also found that VEGFR-2 could be expressed in the infected cells in the injured area. The initial expression began at the limbus, gradually extended to the 1/3 corneal stroma and finally developed into the whole corneal stroma, which was consistent with the location of neovascularization. Studies have shown that inhibition of VEGFR-2 can significantly reduce the formation of new blood vessels<sup>[15-16]</sup>. We used

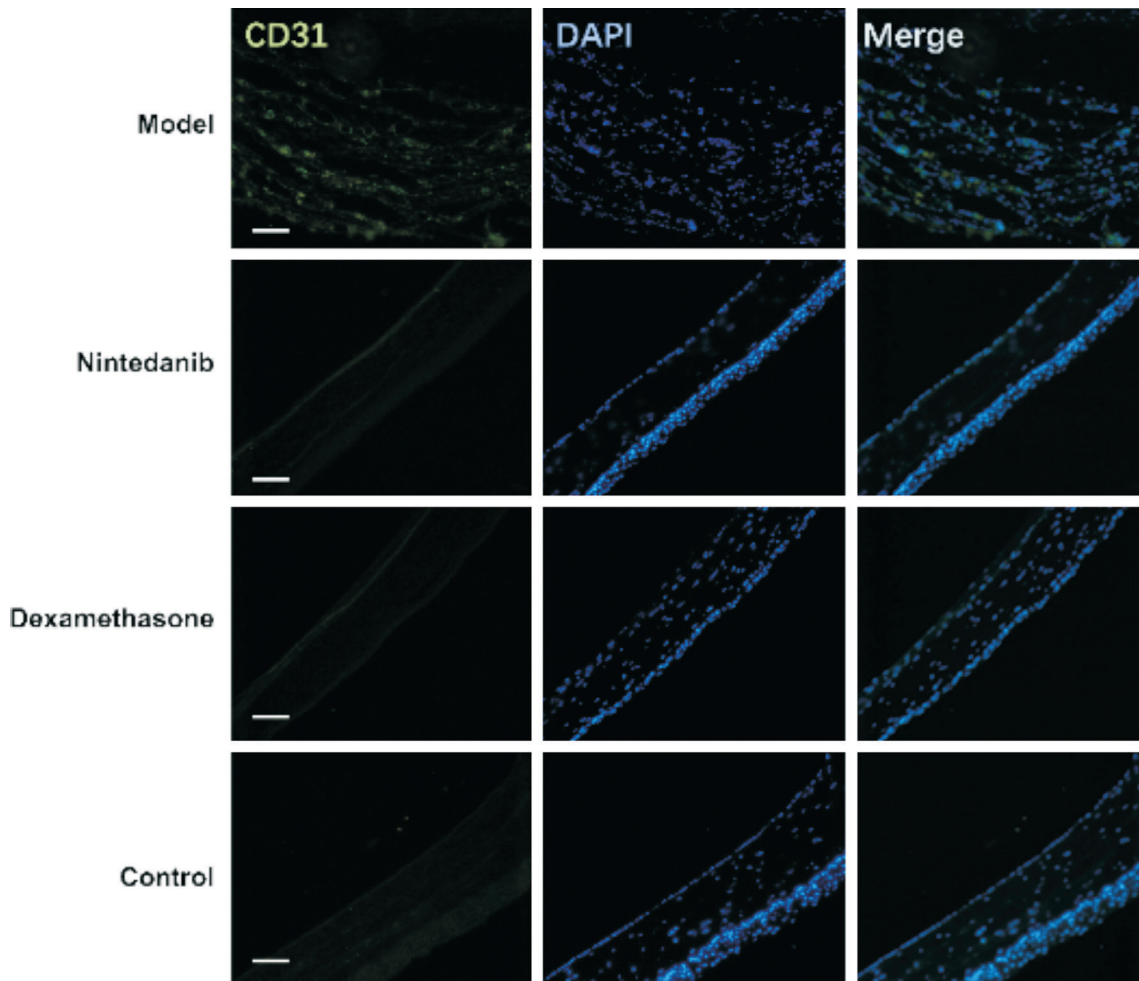


**Figure 5 Immunofluorescence of CD31** Representative CD31 staining images in model, 0.2% nintedanib, 1% dexamethasone, and normal control group at 7d after alkali burn. DAPI was used for nucleus staining. Scale bar=100  $\mu$ m.

immunohistochemistry to detect the expression of VEGFR-2 after corneal alkali burn. The results showed that the expression of VEGFR-2 in the corneal stromal layer of nintedanib group was significantly lower than that of model group ( $P < 0.05$ ). It demonstrated that VEGFR-2 played an important role in neovascularization after corneal alkali burns from another aspect<sup>[16-17]</sup>. The results showed that the area of neovascularization was significantly reduced in the nintedanib groups comparing with the model group, and the inhibition was more pronounced in the 0.2% group.

CD31 can be used to reflect the relative levels of vascular endothelial cells in the cornea, and is often used to evaluate the CNV area. The expression of CD31 in the corneal tissue gradually increases and enters the deep stromal layer<sup>[18]</sup>. The number of cells expressing CD31 gradually decreases after 7d of alkali corneal burn. In the burn group, a higher level of CD31 expression was suggested, indicating a higher level of neovascularization, while its fluorescence level was significantly weakened in the nintedanib group and dexamethasone group<sup>[17-19]</sup>. Combined with the above evidence, further support for nintedanib significantly inhibits CNV,

and these findings also lay the foundation for further clinical research,

In this study, we may conclude that the delivery of nano-thermo-sensitive hydrogel improved the bioavailability of nintedanib and reduced eye complications<sup>[16]</sup>. It is expected to improve medication compliance in clinical applications in the future and create a potential for clinical application. Although the topical application of nintedanib has shown potential advantages in the treatment of CNV, the existence of long-term toxicity remains to be further studied.

#### ACKNOWLEDGEMENTS

**Foundations:** Supported by Zhejiang Province Traditional Chinese Medicine Science and Technology Plan Project (No.2018ZA111); Natural Science Foundation of Zhejiang Province (No.LY19H120001); Zhejiang Provincial Medicine and Health Science and Technology Project (No.2020KY288); Ningbo Natural Science Foundation (No.2019A610353); Ningbo Leading and Outstanding Talents Cultivation Project Selects and Supports Scientific Research Projects (No. NBLJ201801037); Ningbo Public Welfare Science and Technology Plan Project (No.2019C50059); Ningbo Yinzhou

District Science and Technology Bureau Agricultural and Social Science and Technology Plan Project (Yanke [2017] No.110).

**Conflicts of Interest:** Gong Y, None; Wu GH, None; Zhang LY, None; Zhang Z, None; Liao YH, None; Liu XT, None.

#### REFERENCES

- 1 Sharif Z, Sharif W. Corneal neovascularization: updates on pathophysiology, investigations & management. *Rom J Ophthalmol* 2019;63(1):15-22.
- 2 Grossniklaus HE, Kang SJ, Berglin L. Animal models of choroidal and retinal neovascularization. *Prog Retin Eye Res* 2010;29(6):500-519.
- 3 Willoughby AS, Ying GS, Toth CA, Maguire MG, Burns RE, Grunwald JE, Daniel E, Jaffe GJ, Comparison of Age-Related Macular Degeneration Treatments Trials Research Group. Subretinal hyperreflective material in the comparison of age-related macular degeneration treatments trials. *Ophthalmology* 2015;122(9):1846-1853.e5.
- 4 Daniel E, Toth CA, Grunwald JE, Jaffe GJ, Martin DF, Fine SL, Huang JY, Ying GS, Hagstrom SA, Winter K, Maguire MG, Comparison of Age-related Macular Degeneration Treatments Trials Research Group. Risk of scar in the comparison of age-related macular degeneration treatments trials. *Ophthalmology* 2014;121(3):656-666.
- 5 Lu XM, Sun XD. Profile of conbercept in the treatment of neovascular age-related macular degeneration. *Drug Des Devel Ther* 2015;9: 2311-2320.
- 6 Keating GM. Nintedanib: a review of its use in patients with idiopathic pulmonary fibrosis. *Drugs* 2015;75(10):1131-1140.
- 7 Qin S, Li AP, Yi M, Yu SN, Zhang MS, Wu KM. Recent advances on anti-angiogenesis receptor tyrosine kinase inhibitors in cancer therapy. *J Hematol Oncol* 2019;12(1):27.
- 8 Hatano M, Tokuda K, Kobayashi Y, Yamashiro C, Uchi SH, Kobayashi M, Kimura K. Inhibitory effect of nintedanib on VEGF secretion in retinal pigment epithelial cells induced by exposure to a necrotic cell lysate. *PLoS One* 2019;14(8):e0218632.
- 9 Huang HQ, Qi XL, Chen YH, Wu ZH. Thermo-sensitive hydrogels for delivering biotherapeutic molecules: a review. *Saudi Pharm J* 2019;27(7):990-999.
- 10 Giuliano E, Paolino D, Fresta M, Cosco D. Mucosal applications of poloxamer 407-based hydrogels: an overview. *Pharmaceutics* 2018;10(3):E159.
- 11 Dorraj G, Moghimi HR. Preparation of SLN-containing thermoresponsive *in situ* forming gel as a controlled nanoparticle delivery system and investigating its rheological, thermal and erosion behavior. *Iran J Pharm Res* 2015;14(2):347-358.
- 12 Kato T, Kure T, Chang JH, Gabison EE, Itoh T, Itohara S, Azar DT. Diminished corneal angiogenesis in gelatinase A-deficient mice. *FEBS Lett* 2001;508(2):187-190.
- 13 Bhowmik M, Das S, Chattopadhyay D, Ghosh LK. Study of thermo-sensitive *in situ* gels for ocular delivery. *Sci Pharm* 2011;79(2):351-358.
- 14 NL Eremeev VNE, Tsaitler PA. Thermo-sensitive gel for prolongation of ophthalmic drug action. *Journal of Drug Delivery Science and Technology* 2006;16(4):275-278.
- 15 Shibuya M. Vascular endothelial growth factor (VEGF) and its receptor (VEGFR) signaling in angiogenesis: a crucial target for anti- and pro-angiogenic therapies. *Genes Cancer* 2011;2(12):1097-1105.
- 16 Chang JH, Garg NK, Lunde E, Han KY, Jain S, Azar DT. Corneal neovascularization: an anti-VEGF therapy review. *Surv Ophthalmol* 2012;57(5):415-429.
- 17 Voiculescu OB, Voinea LM, Alexandrescu C. Corneal neovascularization and biological therapy. *J Med Life* 2015;8(4):444-448.
- 18 Feizi S, Azari AA, Safapour S. Therapeutic approaches for corneal neovascularization. *Eye Vis (Lond)* 2017;4:28.
- 19 Ormerod LD, Garsd A, Reddy CV, Gomes SA, Abelson MB, Kenyon KR. Dynamics of corneal epithelial healing after an alkali burn. A statistical analysis. *Invest Ophthalmol Vis Sci* 1989;30(8):1784-1793.